The microwave spectrum, *ab initio* analysis, and structure of the fluorobenzene–hydrogen chloride complex

M. Eugenia Sanz, Sonia Antolínez, José L. Alonso, and Juan C. López
Departamento de Química Física, Facultad de Ciencias, Universidad de Valladolid, 47005, Valladolid, Spain

Robert L. Kuczkowski,[a] Sean A. Peebles,[b] Rebecca A. Peebles,[b] and Faith C. Boman
Department of Chemistry, University of Michigan, Ann Arbor, Michigan 48109-1055

Elfi Kraka and Dieter Cremer
Department of Theoretical Chemistry, Göteborg University, S-41320 Göteborg, Reutersgatan 2, Sweden

The fluorobenzene–hydrogen chloride π-hydrogen-bonded complex has been studied by high resolution microwave spectroscopy and *ab initio* calculations. Rotational spectra of the $C_6H_5F-H^{35}Cl$, $C_6H_5F-H^{37}Cl$, and $C_6D_5F-H^{35}Cl$ isotopomers were assigned using pulsed molecular beam techniques in a Fourier-transform microwave spectrometer. The spectra are consistent with a structure of the complex in which the HCl is above the fluorobenzene ring near the ring center, similar to the benzene–HCl prototype dimer. An analysis of the inertial data and the chlorine quadrupole coupling tensor results in two mathematically possible locations for the HCl subunit with respect to the fluorobenzene arising from sign ambiguities in interpreting the spectral constants. One structure has the HCl nearly perpendicular to the aromatic ring; the other has the HCl pointing toward the fluorine end of the ring. Spectral intensities for the μ_a and μ_b transitions favor the former configuration. *Ab initio* calculations (MP2/6-311++G(2df,2pd)+BSSE corrections) indicate that the position of the HCl is driven by electrostatic interactions with the π electrons of the benzene ring. HCl is shifted by 0.16 Å from the center of the ring toward the *para*-C atom, where the π density is significantly higher. In the equilibrium form, HCl is tilted by $\delta=14°$ from perpendicular to the ring with the hydrogen end toward the *para*-C atom. The H atom can perform an internal rotation or at least a half-circular libration (barriers smaller than 100 cm^{-1}). An average δ value of 0.7° is estimated in reasonable agreement with the derived vibrationally averaged value of 3.8°. The complex binding energy ΔE calculated at the CCSD(T)/6-311++G(2df,2pd)+CP(BSSE) level of theory is 2.8 kcal/mol, suggesting a lower ΔE value for benzene–HCl than previously reported. Fluorobenzene–HCl possesses some charge transfer character; however, just 5.5 melectron are transferred from the benzene ring to HCl. In view of this, π–H bonding in fluorobenzene–HCl is predominantly electrostatic rather than covalent in character contrary to claims made in connection with benzene–HCl. © *2003 American Institute of Physics.* [DOI: 10.1063/1.1567714]

I. INTRODUCTION

The interaction of Lewis acids with π electrons to form weakly bonded complexes has received considerable attention, as summarized in a recent study.[1] The family of benzene–HX weakly bonded complexes (X=F,Cl,Br,CN) is particularly interesting, as they exemplify the prototypical aromatic-Lewis acid interaction. Spectroscopic investigations[2–7] concluded that the HX moiety sits above the center of the aromatic ring with the hydrogen pointing to it, which is also in agreement with theoretical predictions.[1,2,8–10] All benzene–HX complexes show sym-

metric top spectra, indicating an effective C_6 symmetry axis in the ground state for the complexes. There are large amplitude motions of the HX in the complexes. A model for these complexes considers mainly the cylindrically symmetric angular oscillation of the HX about its center of mass with the hydrogen atom sampling the π electronic density of the ring. On the basis of this model, the inertial moments and the hyperfine coupling constants indicate that the HX axis is tilted at an average angle of 22°–23° with respect to the benzene C_6 axis for the halides[3,4,6] and 15° for the HCN complex[2] in the ground state. This has led to some discussion in the spectroscopic literature over the years regarding the equilibrium geometry of the complexes. The present consensus seems to be that the ground state average structure (the so-called effective structure) is consistent with C_{6v} symmetry (H pointing to the center of the ring) while the minimum energy configuration of the complex may be one of the

[a]Present address: R. L. Kuczkowski, National Science Foundation, Chemistry Division, Room 1055, 4201 Wilson Blvd., Arlington, Virginia 22230. Electronic mail: rkuczkow@nsf.gov
[b]Present address: Department of Chemistry, Eastern Illinois University, Charleston, Illinois 61920.

equivalent C_s symmetry conformations, where the H atom of the HX is tilted towards a carbon atom or C=C link. Plausible large-amplitude motions can be envisioned averaging to the effective C_6 symmetry axis of the complex in the ground state.

The recent theoretical work concurs with the experimental studies on the basic geometry of the complexes and the existence of a broad, flat potential surface describing the position of the H atom above the carbon ring. Interestingly, a high level calculation[1] for C_6H_6–HCl resulted in a potential surface with a minimum for the HCl tipped 14° to the C_6 axis and a small barrier of 20 cm^{-1} at 0°. The quantum mechanical average position of the HCl resulted in an effective C_6 axis for the complex in the ground vibrational state consistent with the symmetric top spectroscopic character of the complex. An atoms-in-molecules analysis (Bader's formalism) identified six π-type hydrogen bond paths connecting the proton of HCl with each carbon atom in benzene–HCl, also suggesting the possibility of a C_s configuration at the minimum of the potential surface.[8]

It would be interesting to learn how halogen substitution on the benzene ring might affect the geometry of the C_6H_5X–HX complex. There appear to be no high resolution experimental or recent theoretical studies of these species. C_6H_5F–HCl has been studied in cold matrices,[11] and in the gas[11] and liquid phases[12] by infrared spectroscopy, but quantitative structural information is lacking. Of course, the electronic perturbations by fluorine are strong, as exemplified by the electrostatic potential about this substituted aromatic ring.[13,14] This produces a shift in position of an Ar or Ne atom from above the center of the fluorobenzene in the C_6H_5F–Rg (Rg≡rare gas) complexes[15,16] compared to the symmetrical C_6H_6–Rg species.

In this paper we report a high resolution spectroscopic and *ab initio* investigation of C_6H_5F–HCl. The spectroscopic data are consistent with an r_0 average structure of the complex where the HCl is located above the ring, similar to benzene–HCl. Interpretation of the chlorine electric quadrupole coupling constants and the inertial data suggests that in the ground vibrational state the HCl is oriented either nearly perpendicular to the fluorobenzene ring [tipped 4° from perpendicular towards the *para*-carbon (model I, see Fig. 1), or tilted about 49° from the perpendicular toward the fluorine end of the ring (model II, Fig. 1)]. *Ab initio* calculations were undertaken to investigate the potential energy surface of the complex and determine the lowest-energy equilibrium structure, which was found to have the HCl tipped 14° from perpendicular to the ring pointing toward the *para*-carbon atom. This result favors model I for C_6H_5F–HCl. The discrepancy in the tilt angle obtained from the spectroscopic data for HCl is presumably due to the large-amplitude motion of the HCl about its equilibrium position.

II. EXPERIMENTAL DETAILS

The fluorobenzene–HCl complex was generated by supersonic expansion of a gaseous mixture of about 20 mbar of fluorobenzene (Aldrich) and 100 mbar of HCl (Matheson; lecture bottle) in a mixture with Ar up to about 1.5 bar. Fluorobenzene-d_5 (99 atom% D, Aldrich) was used to ob-

serve the C_6D_5F–HCl species. Unsuccessful efforts were made to observe C_6H_5F–DCl using DCl (90 atom% D, Cambridge Isotopes).

The rotational transitions were observed with Balle-Flygare-type Fourier-transform microwave spectrometers[17] (FTMW) at Ann Arbor and Valladolid that have been described previously.[18] The line shapes limited the resolution of the instruments to 10–20 kHz and peak frequencies were reproducible to about 4 kHz for most transitions.

III. SPECTRAL RESULTS AND ANALYSIS

A. Spectra

A model similar to benzene–HCl was used to predict regions to explore the spectrum. The model predicted *b*-dipole and weaker *a*-dipole transitions. After considerable searching an assignment of several *b*-dipole transitions was obtained and the weaker *a*-dipole spectrum was predicted and readily found. The transitions were split into multiplets due to the coupling of the chlorine nuclear electric quadrupole moment with the rotational motion (see Fig. 2). Both the ^{35}Cl ($I=3/2$, 75.5% abundance) and ^{37}Cl ($I=3/2$, 24.5%) isotopomers were assigned. The A-reduced semirigid rotor Hamiltonian of Watson in the I^r representation[19(a)] was fit to the measured transitions. The rotational, quartic centrifugal distortion and quadrupole coupling constants of Table I were determined using the SPFIT global fitting program[19(b)] and the coupling scheme $I+J=F$. The measured transitions and their deviation from the fitted values are given in Table S1 (see supplementary tables[20]).

As discussed below, these two isotopic species predicted two different frequency regions to look for the C_6D_5F–H^{35}Cl species, whose transitions were observed close to one of the predicted sites. The transitions were broadened due to unresolved or partially resolved deuterium quadrupole splitting and the quality of the fit degraded slightly. The C_6D_5F–H^{35}Cl transitions are given in Table S2[20] and the derived constants are in Table I.

B. Structure

Several conclusions were deduced from assigning the C_6H_5F–H^{35}Cl and C_6H_5F–H^{37}Cl species. (1) The initial model was basically correct: the rotational constants are consistent with a structure for the complex where the HCl subunit is located over the fluorobenzene ring; there is a close agreement between the predicted and experimental intensities of the *a*- and *b*-type transitions. (2) HCl lies in the *ab* symmetry plane of the complex that is coincident with the *ac* symmetry plane of fluorobenzene, i.e., the complex has effective C_s symmetry in the ground vibrational state ($P_{bb}=89.23\,u\text{Å}^2$ in free C_6H_5F,[21(a)] $P_{cc}=88.40\,u\text{Å}^2$ in C_6H_5F–H^{35}Cl and 88.39 $u\text{Å}^2$ in C_6H_5F–H^{37}Cl). The location of HCl in the *ab* inertial plane is also consistent with the nonzero value of the off-diagonal element of the Cl–quadrupole coupling tensor χ_{ab} for both C_6H_5F–H^{35}Cl and C_6H_5F–H^{37}Cl, and with the fact that the ratio $^{35}\chi_{cc}/^{37}\chi_{cc}=1.268(3)$ is in excellent agreement with the well-known ratio for $^{35}Q/^{37}Q=1.268\,78(15)$.[19(a)] From the relationship
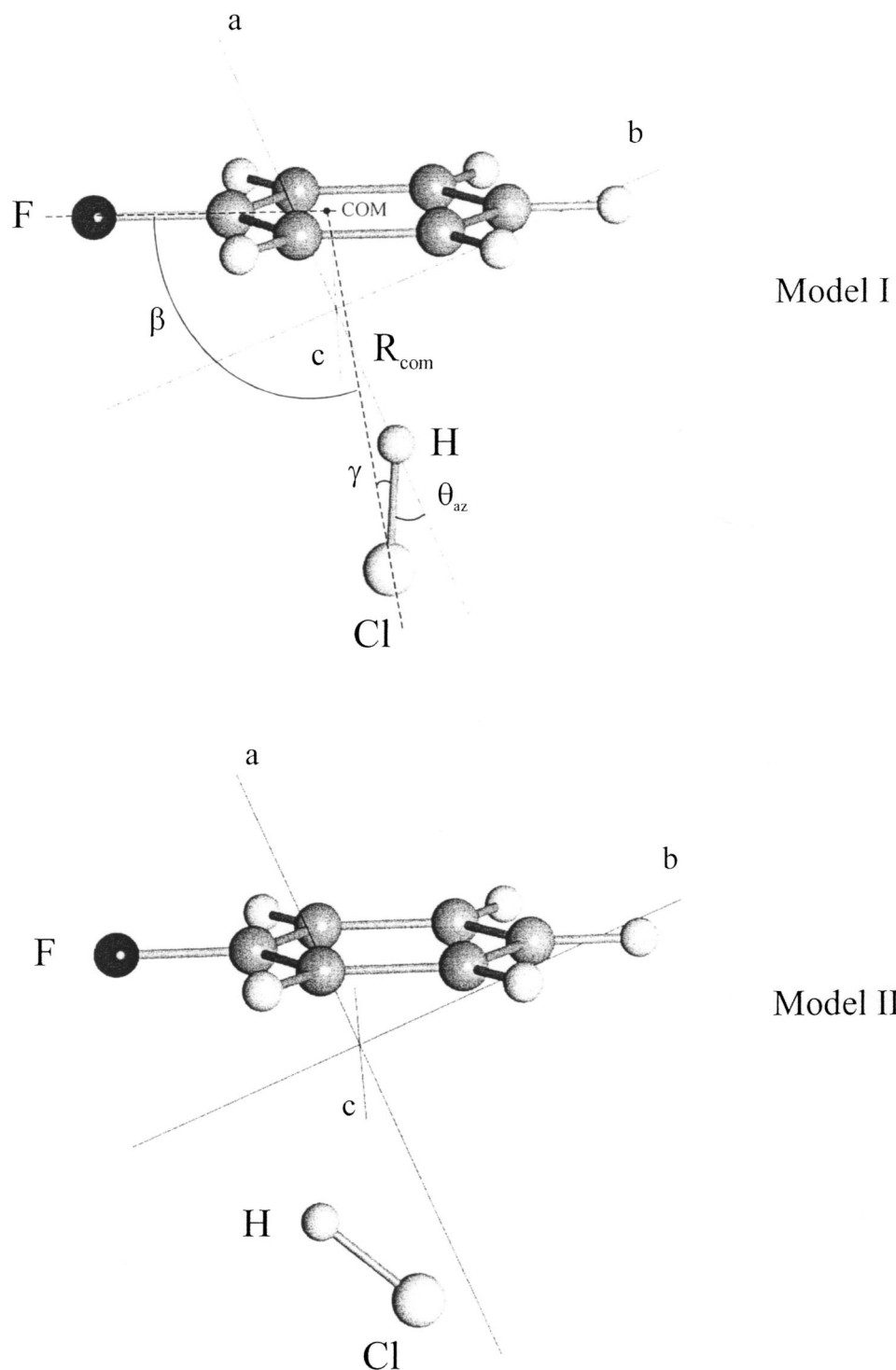
Fluorobenzene-HCl

FIG. 1. The two possible structures of the fluorobenzene–HCl complex consistent with the isotopic experimental data, drawn to scale.

$\theta_{az} = 1/2 \tan^{-1}\{-2\chi_{ab}/(\chi_{aa}-\chi_{bb})\}$, and assuming that the z principal quadrupole axis lies along the HCl bond, the angle θ_{az} between HCl and the a-inertial axis in the complex is calculated to be $26 \pm 0.7°$.

Because the complex has effective C_s symmetry with the HCl above the ring and the C_6H_5F and HCl structures are fixed at their monomer values,[4,21(a)] only three parameters are needed to describe the C_6H_5F–HCl structure. Two of these
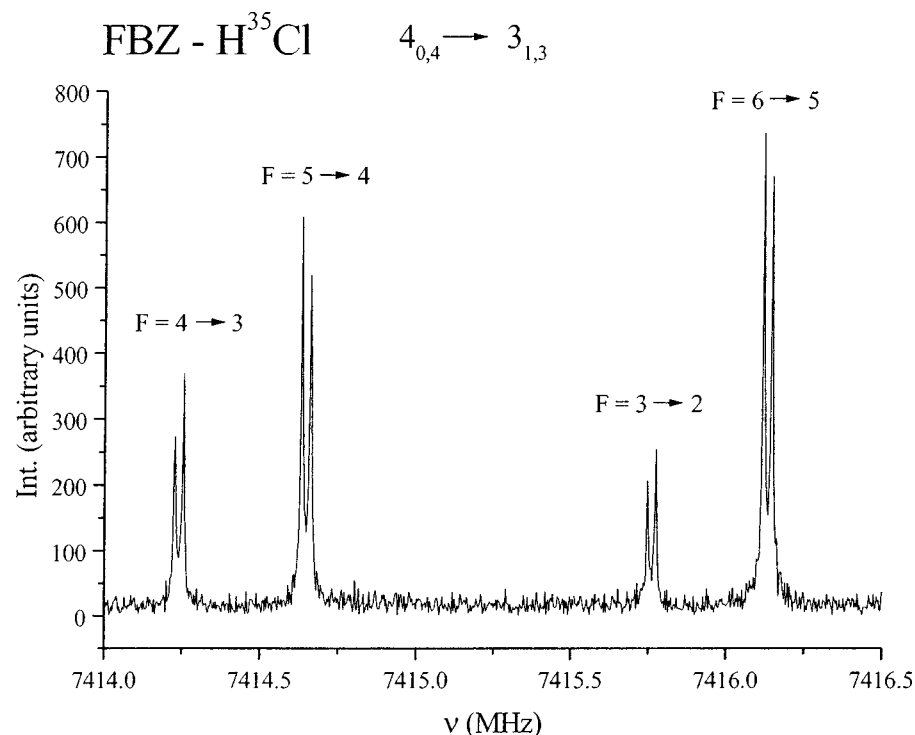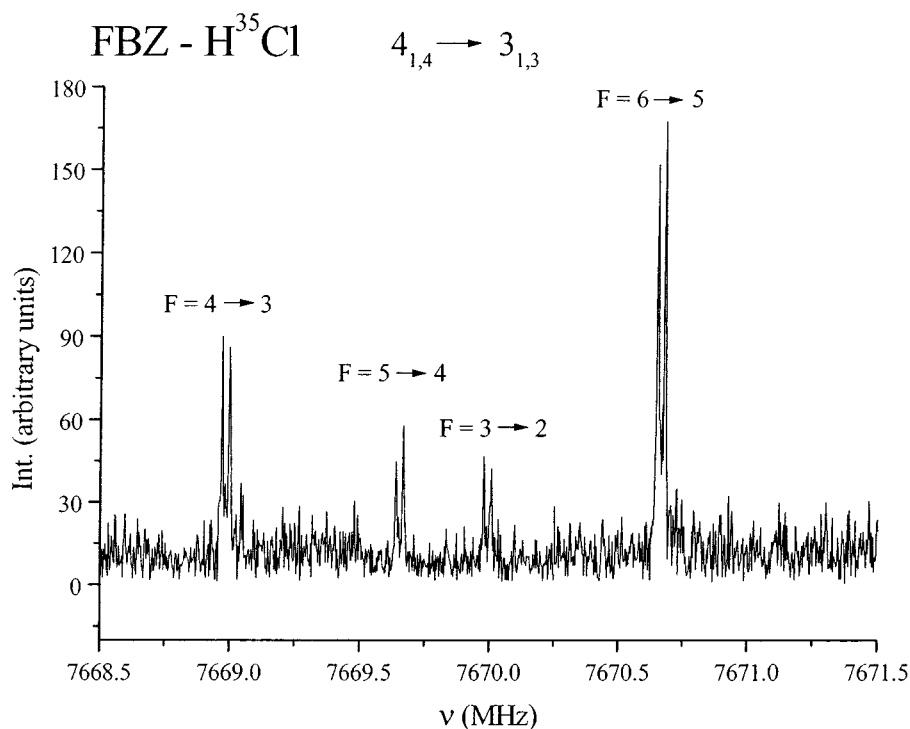
FIG. 2. Observed rotational transitions $J=4_{04}-3_{13}$ (top) and $J=4_{14}-3_{13}$ (bottom), for similar experimental conditions, showing the quadrupole hyperfine components. They are a concatenation of two (top) and three (bottom) files covering 1.5 and 1 MHz each, respectively. F is a half-integer that has been rounded up to the next integer.

are selected to locate the HCl relative to fluorobenzene, for example, the distance R_{com} from the center of mass of fluorobenzene to the Cl atom and the angle β between R_{com} and the C_2 axis in fluorobenzene (see Fig. 1). The third parameter describes the orientation of the HCl axis. We chose either γ in Fig. 1, the angle the HCl axis makes with R_{com}, or, alternatively, θ_{az}, since these are easily parametrized in the inertial fitting program. These can also be transformed to δ,

the angle the HCl axis makes with the perpendicular from Cl to the ring. This angle will be used later in the discussion since it is easier to visualize and relate to electronic effects.

With these parameter definitions an iterative process[21(b),(c)] was employed using least-squares fitting techniques to determine the r_0 structural parameters in Table II. The Michigan version of the STRFIT program was employed.[21(d)] The rotational constants of the ^{35}Cl and ^{37}Cl

TABLE I. Spectroscopic constants for observed isotopomers of fluorobenzene···HCl.

	$C_6H_5F\cdots H^{35}Cl$	$C_6H_5F\cdots H^{37}Cl$	$C_6D_5F\cdots H^{35}Cl$
A/MHz	1863.8635(18)[a]	1860.3155(65)	1655.7079(36)
B	1107.99873(58)	1075.5862(30)	1057.8576(73)
C	918.09242(29)	894.8674(16)	887.8195(263)
Δ_J/kHz	1.7743(79)	1.833(40)	1.572(53)
Δ_{JK}	−0.703(19)	[−0.703][b]	−0.800(125)
Δ_K	2.43(34)	[2.43]	3.29(42)
δ_J	0.5162(34)	0.538(17)	0.4658(33)
δ_K	1.788(10)	4.27(56)	[1.788]
χ_{aa}/MHz	−36.6494(90)	−29.539(50)	−36.3127(87)
$\chi_{bb} - \chi_{cc}$	−14.740(12)	−10.974(36)	−14.905(35)
$|\chi_{ab}|$	30.48(15)	24.6(27)	17.9(65)
N^c	152	79	65
J_{max}.	9	9	7
σ^d/kHz	1.1	1.3	5.7
χ_{bb}/MHz	10.955(11)	9.283(43)	10.704(19)
χ_{cc}/MHz	25.695(11)	20.257(43)	25.609(16)
P_{cc}/u Å^{2e}	88.3992(11)	88.3870(25)	106.8682(104)

[a]Standard error in parentheses in units of the last digit.
[b]Parameters in square brackets were fixed to the $C_6H_5F\cdots H^{35}Cl$ value.
[c]Number of fitted quadrupole components.
[d]Rms deviation of the fit.
[e]$P_{cc} = (I_a + I_b - I_c)/2 = \Sigma\, m_i c_i^2$. Conversion factor: 505379.1 MHz uÅ^2.

TABLE II. Structural parameters of fluorobenzene···HCl.[a]

	Model I	Model II	MP2/6-311++G(2df,2pd) +CP(BSSE)
Fitted parameters			
R_{com}	3.700(2)	3.694(2)	3.701
β	100.7(2)	101.2(2)	100.0
γ	14.5	−37.5	16 (24)[b]
Derived parameters			
$R_{Cl,F}$	4.647	4.656	4.626
$R_{H,F}$	3.795	3.400	3.967
$R_{Cl,ClP}$	3.635	3.623	3.645
$R_{H,HP}$	2.456	2.675	2.400
u	0.162	0.191	0.116
δ	3.8	−48.7	0.7(14.0)[b]
ΔI_{rms} (μ Å^2)[c]	0.59	0.59	

[a]Distances are in Å, angles in degrees. R_{com} is the distance between the center of mass of fluorobenzene and the Cl atom; β is the angle ∠F-com-Cl (com is the center of mass of fluorobenzene); γ is the angle ∠com-Cl–H, fixed to give the α_{az} angle determined from the quadrupole data; $R_{X,XP}$ is the perpendicular distance of X to the ring (see Fig. 3); Distance u is the shift of Cl, parallel to the ring from the geometric center of the ring, toward C_4; δ is the angle ∠H–Cl–ClP between H, Cl, and the perpendicular from Cl to the ring.
[b]The first entry gives the estimated average value while the value in parentheses is the equilibrium value.
[c]ΔI is $I_{calc} - I_{obs}$ derived from the least squares fitting of the experimental I's to the observed structures.

species effectively determine R_{com} and β, or, more precisely, the $|a_{Cl}|$ and $|b_{Cl}|$ coordinates in the inertial axis system. If one makes the plausible assumption that the H end of HCl is directed toward C_6H_5F, there are four models consistent with the ^{35}Cl and ^{37}Cl rotational spectra due to the sign ambiguities for the chlorine coordinates and for the orientation angle (θ_{az}) of the HCl estimated from the quadrupole coupling data. Two of these correspond to the chlorine atom lying 3.62–3.63 Å above the ring between the C_6H_5F center-of-mass and C4 (*para*-carbon), with the HCl axis nearly perpendicular to the ring (model I, Fig. 1) versus tilted from perpendicular about 49° toward the fluorine (model II). The other two have similar configurations but place the chlorine between the C_6H_5F center of mass and Cl (fluorinated carbon), again with the HCl axis nearly perpendicular to the ring (III) versus tilted toward the fluorine (IV). These models predicted isotope shifts for the C_6D_5F–$H^{35}Cl$ species of 208, 51, and 31 MHz (ΔA, ΔB, ΔC, respectively) for I and II, and 186, 67, and 36 MHz for III and IV. The observed values of 208.16, 50.13, and 30.28 MHz were only consistent with models I and II.

These three observed isotopic species effectively locate the chlorine relative to the fluorobenzene, but the inertial information is insufficient to locate precisely the light H atom of HCl. However, using the quadrupole coupling data to fix the HCl orientation at $|\theta_{az}| = 26.0°$ in the fit, this converges to the parameters of Table II (illustrated in Fig. 1), which are consistent with structures I and II. The principal axis coordinates consistent with these fits are given in Table S3.[20] An analysis of the fitted structures indicates that the HCl axis is nearly perpendicular to the fluorobenzene plane in I. More precisely, it is tipped about 4° ($\delta = 3.8°$; see Fig. 3) toward the *para*-carbon atom. In II, it is tipped 49° ($\delta = 48.7°$) toward the fluorine end. However, these structural

parameters are affected by the use of ground state moments in conjunction with fixing θ_{az}. It is difficult to estimate how these parameters may compare to the equilibrium values. Based on their sensitivity (or insensitivity) in the fitting, these so-called effective (r_0) values of R_{com}, β and γ (or δ) should be within about 0.05 Å, 5°, and 10°–15°, respectively, of the equilibrium values.

The discrimination between I and II may be possible by assignment of the C_6H_5F–DCl isotopomer, although the expected isotope shifts are smaller (I: 0.0, 5.3, and 3.6 MHz for ΔA, ΔB, and ΔC, respectively; II: 8.1, 5.3, and 5.7 MHz) and vibrational averaging effects upon deuteration could be significantly different than in the HCl species and introduce ambiguities. After exhaustive searches, no transitions that could be attributed to the C_6H_5F–DCl species were observed. Significant deuterium exchange problems as monitored on HCl–Ar and DCl–Ar transitions complicated this search and deuterium quadrupole splitting effects probably also reduced the intensity of the transitions.

We next explored relative intensity measurements of the *a*- and *b*-dipole transitions, since this has the potential to provide some structural insights. An effort was made to compare the intensities of the transitions $J = 4_{04} - 3_{13}$, $F = 11/2 - 9/2$ at 7416.13 MHz and $J = 4_{14} - 3_{13}$, $F = 11/2 - 9/2$ at 7670.66 MHz, although intensity comparisons are a tricky endeavor in FTMW spectrometers. The amplitude spectra in the frequency domain (presumably for $\pi/2$ conditions) were compared in a series of runs for this transition pair, where the temperature of the molecular beam is not a factor (see, e.g., Fig. 2). This resulted in a ratio for μ_b / μ_a of 3.3 ± 1.5. Using the dipoles of 1.555 D[15] and 1.108 D[22] for fluorobenzene and HCl, respectively, and assuming that polarization

effects can be ignored, structure I predicts μ_b/μ_a = 1.93/0.40 = 4.8. The fluorobenzene and HCl dipoles more nearly cancel along the b axis in II, resulting in μ_b/μ_a = 0.95/0.35 = 2.7. This would seem to favor the structure with HCl tilted to the fluorine. However, polarization effects are likely not to be negligible. In benzene–HCl, the calculated dipole moment of the complex is estimated to be 0.7–0.9 D greater than in free HCl.[1] If an induced dipole moment of 0.5 D along the HCl axis is added to the HCl moment, the predicted components change to μ_b/μ_a = 2.15/0.85 = 2.53 for I and 0.85/0.72 = 1.2 for II. Thus, the intensities suggest that a structure with HCl pointing to the fluorine is not reasonable. In order to be confident of this conclusion, considerably more work on several other pairs of transitions for different spectroscopy conditions would be necessary, along with a more careful consideration of the crude polarization

model and vibrational averaging effects. Nevertheless, this result definitively eliminates configurations with the proton in HCl pointing away from the ring, since they predict $\mu_a \geqslant \mu_b$.

IV. QUANTUM CHEMICAL INVESTIGATION

The quantum chemical study was carried out parallel to the experimental investigation to obtain an independent description of the complex. Although there is convincing experimental evidence that benzene–HCl represents a π–H bonded complex with effective (vibrationally averaged) C_{6v} symmetry,[4,5,7] such a structure cannot be *a priori* assumed for fluorobenzene–HCl. A σ–H bonded complex (H bond toward F) is similarly likely. Several structural possibilities (see Scheme 1)
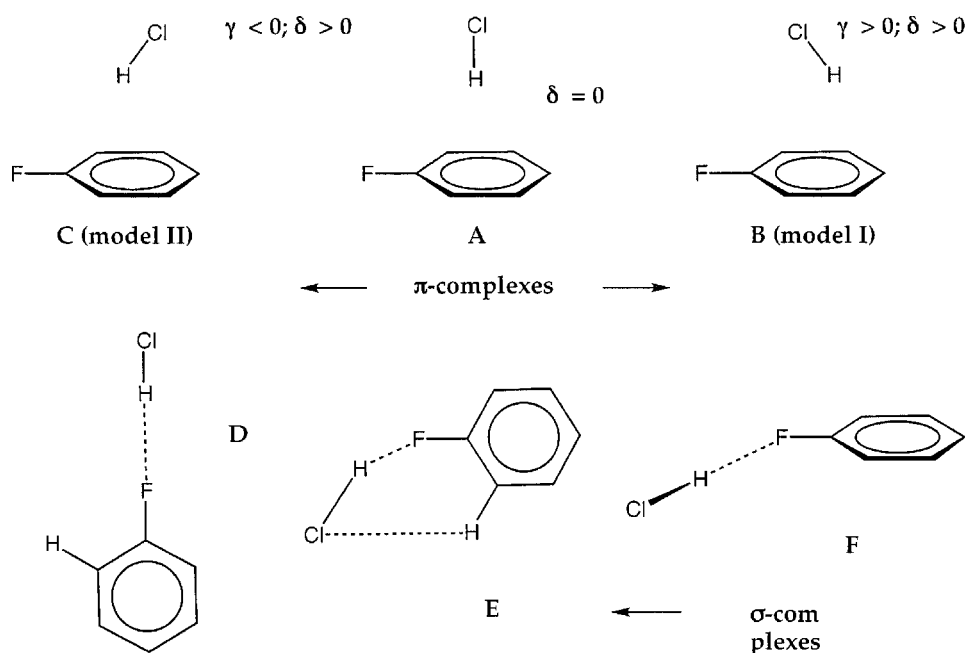
were tested, namely π complexes **A** ($\delta = 0$, HCl perpendicular to the ring), **B** ($\delta > 0$, H toward C4, corresponding to model I), **C** ($\delta > 0$, H toward F, corresponding to model II), and σ complexes **D** (C_{2v} symmetry), **E** (C_s symmetry), and **F** (C_1 symmetry).

Both second-order Møller–Plesset (MP2) perturbation theory[23] and Coupled Cluster theory, including all single and double excitations and a perturbative inclusion of all triple excitations [CCSD(T)][24] were applied to describe the complex. First calculations were carried out with a 6-31G(+sd, +sp) basis designed by Spackman[25,26] to provide a reasonable account of dispersion interactions. For a better description of the complex, we used in the second step of the investigation Pople's VTZ basis 6-311++G(2df,2pd),[27] which contains a set of diffuse sp functions on all heavy atoms, diffuse s functions on H, and in addition is augmented by 2d and 1f functions in the heavy atoms basis sets thus

leading to 370 functions for fluorobenzene–HCl. This basis is known to provide a reasonable account of both dispersion and electrostatic interactions in van der Waals complexes when applied at the MP2 level of theory (compare, e.g., with the MP2/6-311++G(3df,2p) calculations performed for benzene–HCl in Ref. 1).

The fluorobenzene–HCl complex was described by determining its equilibrium geometry, complex binding energy, and electron density distribution $\rho(\mathbf{r})$. All calculations (geometry optimizations, density investigations, and calculations of other molecular properties) were carried out, including systematic corrections for basis set superposition errors (BSSEs)[28] along the lines described previously.[29,30] For this purpose, the counterpoise procedure (CP) of Boys and Bernardi[31] was used, which employs the dimer-centered basis sets (DCBS) for all monomer calculations. This level of

theory is abbreviated in the following as Method/basis +CP(BSSE).

The electron density distribution was analyzed with the help of difference electron density distributions $\Delta\rho(\mathbf{r})$ $=\rho(\text{complex})-\rho(\text{HCl,DCBS})-\rho(\text{benzene}-\text{F,DCBS})$, where the density of the monomers was determined using the complex geometry for the position of the ghost functions describing the influence of the basis of the second monomer. All densities were calculated as MP2 response densities using either the 6-31G(+sd,+sp) or the 6-311++G(3df,2p) basis set. The analysis of the density distribution was complemented by the calculation of natural bond orbitals (NBOs) and natural atomic orbital (NAO) charges, again employing MP2 response densities.[32] The NBO/NAO analysis has proven to be superior to a Mulliken analysis, and therefore leads to a more realistic description of charge transfer complexes. All calculations were carried out using the COLOGNE2000[33] and ACESII[34] *ab initio* packages.

Preliminary calculations at the MP2/6-31G(+sd,+sp) level of theory suggested that structure **B** ($R_{\text{com}}=3.720$ Å, $\gamma=14.2°$, $\beta=101.6°$) is more stable than either **A** or **C**. Structures **D** and **E** turned out to be higher-order saddle points (**D**:$\Delta E=-0.43$ kcal/mol, $283i$, $34i$, $13i$; **E**:$\Delta E=-0.92$ kcal/mol, $67i$, $19i$) while structure **F** turned out to be the global minimum ($\Delta E=-1.02$ kcal/mol; all ΔE values relative to **A**). However, when BSSE corrections were included at the MP2/6-31G(+sd,+sp)+CP(BSSE) level of theory, structure **B** changes its geometry considerably, yielding $R_{\text{com}}=3.817$ Å, $\gamma=28.9°$, $\beta=97.7°$, and a (stabilizing) complex binding energy $\Delta E(\text{complex})=2.68$ kcal/mol (given relative to the energy of the monomers). Also, structure **F** turned out to be unstable (HCl dissociation leading to protonation at F). These results clearly document the importance of BSSE corrections in line with many previous results.[29,30,35]

The relatively large discrepancy between experimental and calculated R_{com} (calc: 3.82 Å; expt: 3.70 Å) and γ values (calc: 28.9°; expt: 14.5°) suggests that the use of relatively small basis sets optimized for describing dispersion-dominated complexes (benzene–Ar, etc.[36]) may not be sufficient to describe van der Waals complexes stabilized by pronounced electrostatic interactions. MP2/6-311++G(2df,2pd) +CP(BSSE) calculations led to $R_{\text{com}}=3.701$ Å, in good agreement with the experimental value of 3.700 Å, suggesting that the VTZ+diff basis augmented by f functions is appropriate to describe the complex structure. This was also confirmed by the calculated β value (100.0° vs 100.7° derived from experiment). However, the deviations between the experimental γ value of 14.5° and the computed value (reduced to 24.0° with the larger basis set) remained.

MP2/6-311++G(2df,2pd) calculations for alternative models II, III, and IV (see Sec. III B) all confirmed that structure **B** (model I) derived from the measured data provides the correct description of the π complex. The σ complex possessing the structure of **D** was found to present a minimum [contrary to **E** and **F**, which are not located at stationary points of the MP2/6-311++G(2df,2pd)+CP(BSSE) potential energy surface (PES)] possessing, however, a complex binding energy substantially smaller than that of π complex

B. Hence, σ H bonding in fluorobenzene–HCl was not further investigated.

The binding energy of the π complex calculated with the larger basis set increases to 3.67 kcal/mol relative to the energy of the monomers. A CCSD(T)//6-311++G(2df,2pd) +CP(BSSE) calculation leads to 2.83 kcal/mol. Both values compare well with the range of binding energies $1.8<D_0<3.8$ kcal/mol obtained by dispersed fluorescence spectra for benzene–HCl[5] but are somewhat smaller than $D_0=4.79\pm0.12$ kcal/mol determined for benzene–HCl by photoionization threshold measurements.[7] Since the binding energy for fluorobenzene–HCl should be similar to that of benzene–HCl (actually one should expect that it is slightly larger; see below), and since vibrational corrections hardly change the binding energy, the CCSD(T) calculations give a clear preference for a D_0 (benzene–HCl) value close to 3 kcal/mol, in line with the results from dispersed fluorescence spectra[5] and in disagreement with the photoionization experiments[7] and recent *ab initio* calculations.[1] We note in this connection that the BSSE corrections reduce calculated binding energies by 1.4 (large basis)–4.5 kcal/mol (small basis) and, therefore, are essential for the calculation of D_e or D_0. The detailed analysis of the BSSE corrections reveals that it is very important to have d-type polarization functions at the H atoms (in particular, that of HCl) and f-type polarization functions at the C and Cl atoms. They reduce the BSSEs considerably. Nevertheless, it is revealing that 57% (42%) of the BSSE corrections are due to the HCl part of the complex when using the large basis set (small basis set).

V. DISCUSSION

The geometry of fluorobenzene–HCl is discussed using the parameters R_{com}, u [distance between Cl projected (ClP) and geometrical center of the ring (GCR)], ν [distance between H projected (HP) and ClP], and the angles β, γ, δ [Fig. 3(a)]. For the description of a possible rotation of HCl above the benzene ring, we use a cylindrical coordinate system established by the angle δ (equivalent to a radial parameter) and the phase angle ϕ [Fig. 3(b)].

The Cl atom is shifted by the distance u (exp: 0.162 Å; calc: 0.116 Å) from the GCR toward the *para*-C atom (C4). This is just opposite to the shift found for fluorobenzene–Ar ($u=-0.297$ Å[15]) and reflects the fact that the latter complex is stabilized predominantly by dispersion forces, while in the complex fluorobenzene–HCl electrostatic interactions prevail. As was discussed in Refs. 29 and 36, Ar approaches the benzene from above so that the best compromise between (destabilizing) exchange repulsion interactions and (stabilizing) dispersion interactions is achieved. In benzene, the approach line would be exactly along the C_6 symmetry axis because in this direction there is a hole in the exchange repulsion sphere enveloping the benzene molecule. Ar can approach benzene as closely as possible and establish dispersion interactions with the π clouds of all six C atoms at the same time.

In fluorobenzene, the π density is contracted at the side of the *ipso*-C atom (C1) contracting in this direction the surface of destabilizing exchange repulsion interactions. Ar is shifted slightly toward C1 to approach the ring closer
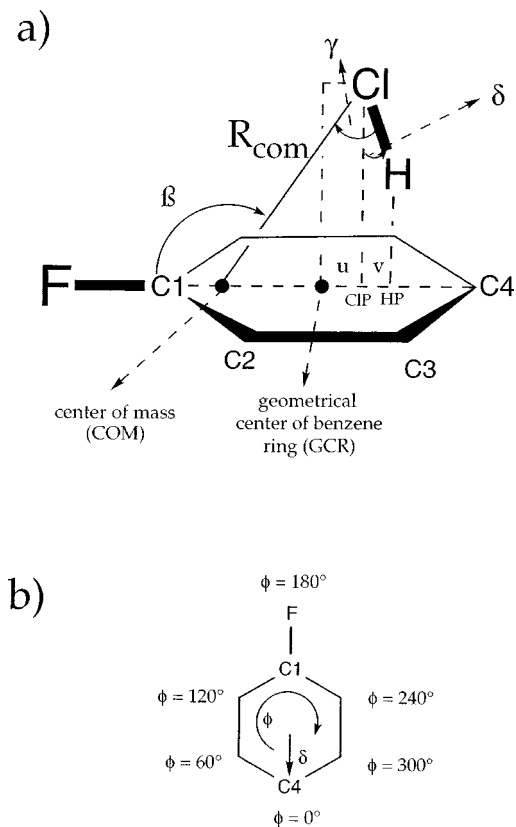
FIG. 3. The definition of the geometrical parameters used in the description of fluorobenzene–HCl. (a) Distance R_{com} connects the Cl atom with the center of mass of fluorobenzene. The points HP and ClP give the projections of HCl into the plane of the ring. Length u and $u+v$ shift the Cl and the H atom from the GCR (geometrical center of the ring) toward C4. The angle β is the angle between the CF bond axis and R_{com}. The angle γ is the angle between R_{com} and the ClH bond axis. Angle δ measures the deviation of the ClH bond axis from the perpendicular direction given by Cl,ClP. In the mirror plane of the complex, δ is given by $\delta = \gamma + 90 - \beta$. Note that γ can adopt positive and negative values while δ is always positive. (b) The internal rotation of the HCl molecule is described by the phase angle ϕ and the angle δ, which takes the role of a radial parameter. Angle δ varies for $\phi = 0°$ to 360°.

and benefit more from stronger stabilizing dispersion interactions. This is reflected by the difference electron density distribution $\Delta\rho(\mathbf{r}) = \rho(\text{fluorobenzene–Ar}) - \rho(\text{Ar,DCBS}) - \rho(\text{fluorobenzene,DCBS})$ shown in Fig. 4(a). The value of $u < 0$ results from the fact that the Ar atom takes advantage of the extension of the "exchange repulsion hole" in the direction of C1 while keeping at the same time dispersion interactions with the other five C atoms of the benzene ring. These considerations will apply also if HCl approaches the ring with the Cl atom first.[37] If HCl approaches the benzene ring with the H atom first, exchange repulsion plays a smaller role because the electron of the H atom is largely drawn into the bond region of HCl and the electronegativity difference between H and Cl reduces the density at the side of the H atom even further. The H atom is partially positively charged and accordingly it is attracted by the π cloud of the benzene ring. Due to the π-donor capacity of F, the π charges are higher in ortho- and para positions of the ring (C1: -3.8 me; C2: -34.5 me; C3: $+2.6$ me; C4: -18.1 me; values <0 indicate an increase of the π- density of 1.000 e).
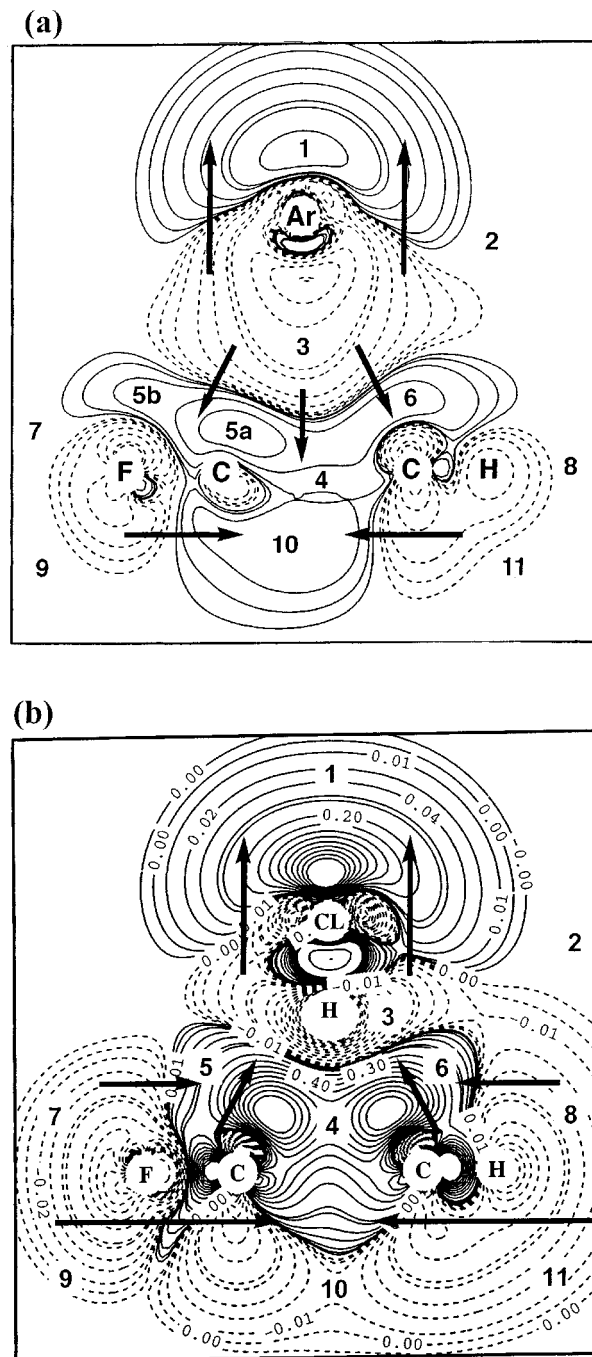

FIG. 4. Contour line diagram of the MP2 difference electron density distribution of (a) fluorobenzene–argon and (b) fluorobenzene–HCl (for $\delta = 0°$) calculated with a $[7s4p2d1f/4s3p1d/3s1p]$ basis at optimized geometries. The Cl atom is centered over the geometrical center of the ring (GCR) for reasons of comparison with the fluorobenzene–argon complex. The reference plane is the plane perpendicular to the benzene ring that contains Ar(HCl) and the C1–F/C4–H bonds. Contour lines range from 2×10^{-6} to 2×10^{-1} (e/Bohr^3). Solid lines correspond to an increase of electron density upon complex formation, dashed lines to a decrease. Regions of increase and decrease of electron density are marked by small numbers. Arrows give the direction of charge polarization, as discussed in the text.

Also, the π-density becomes more diffuse toward C4 due to the rapidly decreasing σ-withdrawing effect of F, influencing, in particular, C1. Hence, an increase in electrostatic attractions can be accomplished by HCl shifting toward C4 by distance u. There are two possibilities to further maximize

electrostatic interactions between HCl and the benzene ring: (a) HCl "rides" on the π cloud of the half-circle formed by (C2–C3–C4–C5–C6) (large value of u). (b) The Cl atom "rests" at a more central position and the Cl–H bond is tilted toward the peripheral C atoms so that the H atom swings around the Cl atom again following the half-circle C2–C3–C4–C5–C6 in an oscillatory motion. Clearly, possibility (a) is dynamically unfavorable because of the large mass of the Cl atom. A half-circular motion of the H atom while the Cl atom keeps essentially its position is more likely.

In Fig. 4(b), a contour line diagram of the MP2 difference electron density distribution $\Delta\rho(\mathbf{r})$ of the fluorobenzene–HCl complex is shown for structure **A** ($\delta=0$, Scheme 1) so that a direct comparison with that of fluorobenzene–Ar [Fig. 4(a)] is possible. The reference plane is the plane containing HCl, C1–F, and C4–H. As found for the van der Waals complex fluorobenzene–Ar, there is a regular pattern of regions with increase (solid contour lines) and decrease (dashed contour lines) of electron density caused by complex formation. Exchange repulsion between the Ar atom and the benzene ring leads to charge polarization for both monomers: a large region of charge depletion [Fig. 4(a), region 3) is enclosed by smaller, compressed regions of charge increase directly in front of Ar (region 2) and in the π region of benzene (regions 5 and 6). Negative charge is pushed to the back of the Ar atom (region 1) and through the center of the benzene ring to the backside of the molecule (region 10).

A similar charge polarization can be observed for the fluorobenzene–HCl complex [Fig. 4(b)]: the H atom is largely depleted of density, bonding density is pushed toward the Cl atom, and negative charge of the Cl atom is pushed to its back [region 1, Fig. 4(b)] where a large accumulation of density can be found similarly as in the case of the Ar atom. The differences with regard to the Ar complex are seen in the intermolecular region: π density of the benzene ring is drawn into this region [regions 4, 5, 6 in Fig. 4(b)] thus substantially decreasing the region of charge depletion. Hence, the difference density clearly reflects the fact that the positively charged H atom (region 3) attracts π density from the benzene ring while the opposite is true in the case of the Ar complex.

From Fig. 4 it becomes obvious that F loses both σ and π density in the fluorobenzene–HCl complex (i.e., the π-donor capacity of F is enhanced, its σ-acceptor capacity reduced), while in the corresponding Ar complex the π density of the F atom is largely preserved. Also, the π density of the C atoms is drawn from below the ring into the intermolecular region [see the arrows in Fig. 4(b)]. σ density is drawn into the center of the benzene ring and up toward the HCl molecule.

The preference for the HCl aligned with the H atom toward C4 ($\delta>0$, $\phi=0°$) becomes clear when considering the directions of charge polarization and charge withdrawal reflected by Fig. 5(a), which gives the difference electron density distribution for structure **B** (Scheme 1). If the H atom of HCl points toward C4, it will particularly draw π density of the latter atom into the intermolecular space, thus further enhancing the natural π-donor capacity of the F atom (ac-
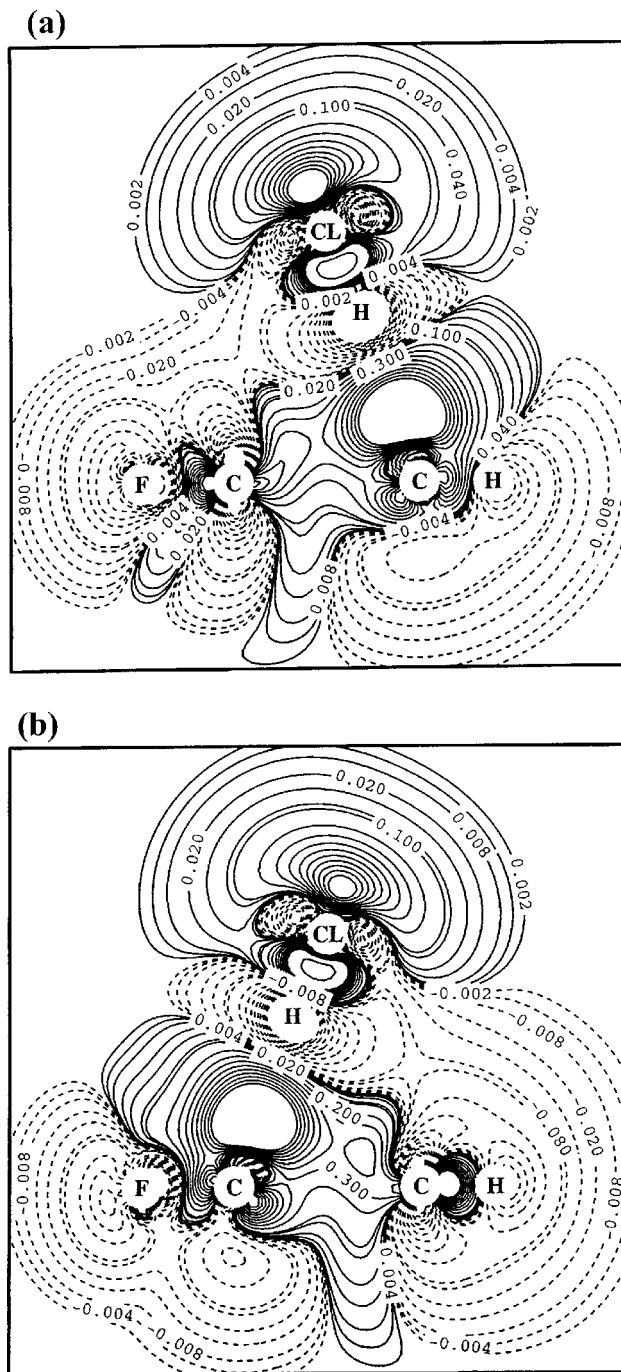

(a)

(b)

FIG. 5. Contour line diagram of the MP2 difference electron density distribution of fluorobenzene–HCl for two positions of HCl: (a) $\phi=0°$ and $\delta=14°$ ($\gamma=24°$); (b) $\phi=180°$ and $\delta=14°$ ($\gamma=-4°$). The Cl atom is centered over the GCR for reasons of comparison with Fig. 4. The reference plane is the plane perpendicular to the benzene ring that contains HCl and the C1–F/C4–H bonds. Contour lines range from 2×10^{-6} to 2×10^{-1} (e/Bohr^3). Solid lines correspond to an increase of electron density upon complex formation, dashed lines to a decrease.

cording to the NBO analysis the total charges of C3 (C5) and C4 increase by 8 and 19.9 melectron, respectively, while those of C1 and C2 (C6) decrease by 3.9 and 3.6 melectron, respectively). This is a complex stabilizing interaction. If, however, the H atom and the HCl bond point toward the *ipso*-C atom, C1 (structure **C**, $\delta>0$, $\phi=180°$, Scheme 1), or even to the F atom (model II), π density will be drawn from
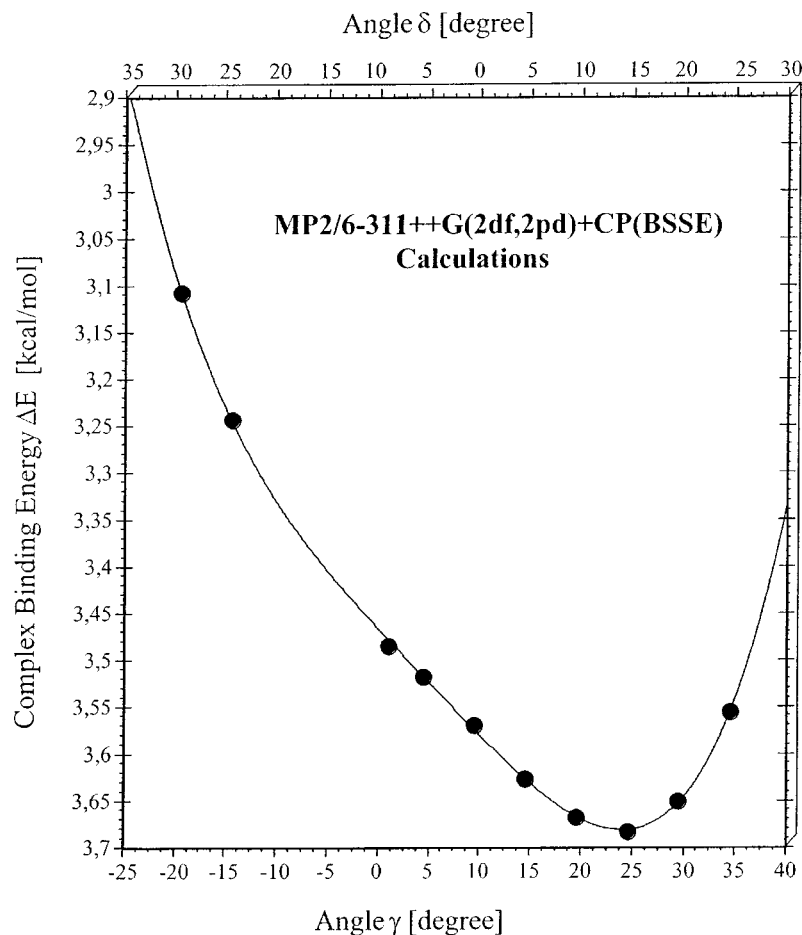
FIG. 6. The complex binding energy calculated at the MP2/6-311++G(2df,2pd)+CP(BSSE) level of theory is given as a function of the inclination angles δ (top scale) and γ (bottom scale).

the *ortho*-C atoms and the *para*-C atom back to the CF atom thus reversing the natural π-donor capacity of F [Fig. 5(b)]. Since the benzene ring with its low-lying π^* MOs is a better π acceptor than the F atom (an increase of the number of valence electrons beyond 8 is highly destabilizing), any value of δ with H pointing toward F ($\phi=180°$) leads to a destabilization of the fluorobenzene–HCl complex. Actually, changes in the density upon complex formation seem to be similar for structure **B** [$\delta>0$, $\phi=0°$, H toward C4, Fig. 5(a)] and structure **C** [$\delta>0$, $\phi=180°$, H toward C1, Fig. 5(b)]. However, these changes have to be seen on the basis of the absolute atomic charges of fluorobenzene before complex formation. At this stage C1 is strongly positively charged (+411 melectron) while C4 has a negative partial charge (−211 melectron) according to the NBO+CP/BSSE analysis. Hence, structure **B** ($\delta>0$, $\phi=0°$, H toward C4, model I) leads to the electrostatically more favorable situation.

A. The motion of the HCl molecule

In benzene–HCl, the HCl molecule undergoes an internal oscillation with the H atom gliding over the π density of the benzene ring. This is in line with a measured average angle δ of 23°.[4,5] A similar motion should take place in the fluorobenzene–HCl complex where, however, two additional effects not present in the benzene–HCl complex play an important role: (a) the fluorobenzene–HCl complex has effective C_s symmetry; (b) the potential for a movement of HCl in the effective mirror plane of the complex is asymmetric. The

latter effect is responsible for a shift of the Cl atom toward C4. This leads to a δ value of 14° ($\gamma=24.0°$ for $\beta=100.0°$, Table II), as becomes obvious from MP2/6-311++(2df,2pd)+CP(BSSE) calculations.

The shift of the position in the Cl atom from the ring center toward C4 is responsible for the fact that the circular motion of the H atom is strongly distorted. Describing this motion by phase angle ϕ and the conical angle δ [Fig. 3(b); note that δ is always $\geq 0°$ while γ can adopt both positive and negative values], the angle ϕ is 0° (60°, 120°) for H pointing toward C4 (C3,C2) and increases to 180° for H pointing toward C1 [Fig. 3(b)]. Using MP2/6-311++(2df,2pd)+CP(BSSE) theory, we have varied $\delta(\gamma)$ for given values of ϕ [$\phi=0°$ (180°), $\phi=60°$ (240°), $\phi=90°$ (270°), etc.] to determine the value of $\delta_{opt}(\gamma_{opt})$ for which the complex binding energy adopts a maximum. Figure 6 gives the changes in the complex binding energy ΔE for a variation of $\delta(\gamma)$ along the direction of $\phi=0°$ (180°) while Fig. 7 gives the variation in ΔE for an internal rotation ($\phi=0°$ to $\phi=360°$) using for each ϕ value investigated that angle $\delta_{opt}(\gamma_{opt})$ that leads to the maximum ΔE.

Both Fig. 6 and Fig. 7 reveal that the PES calculated at the MP2/6-311++(2df,2pd)+CP(BSSE) level of theory is extremely flat for {$0°\leq\phi\leq360°$; $-20°<\gamma<35°$} varying by less than 0.6 kcal/mol. The minimum of the PES is located at {$\phi=0°$, $\delta=14.0°$, $\gamma=24.0°$}, i.e., the equilibrium geometry of fluorobenzene–HCl possesses C_s symmetry. The PES is
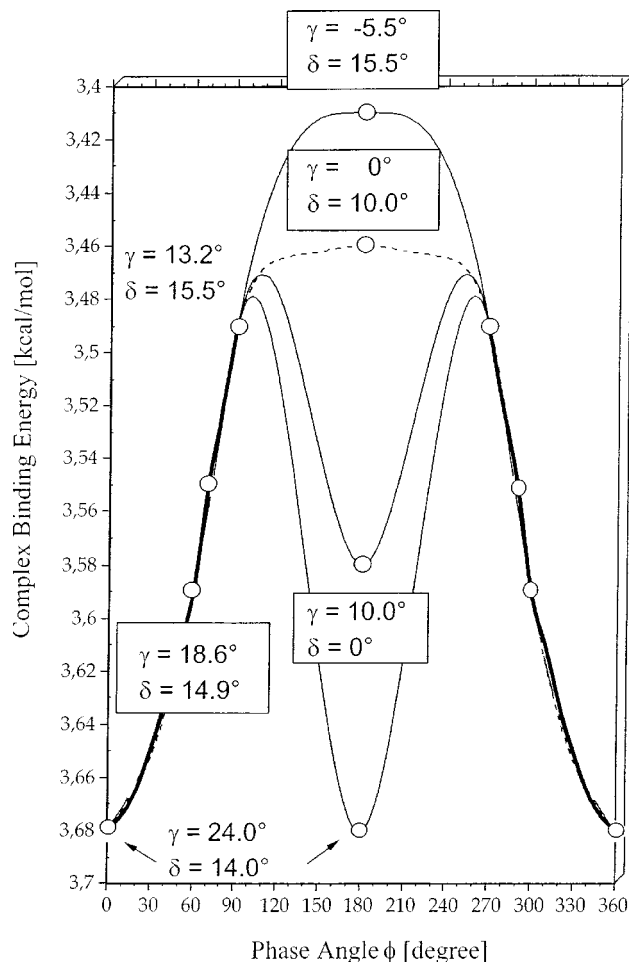
FIG. 7. The complex binding energy calculated at the MP2/6-311 ++G(2df,2pd)+CP(BSSE) level of theory is given as a function of the phase angle ϕ. For selected points, the optimized values of inclination angles γ and δ are given. The bold line indicates the ϕ region of a large-amplitude libration while the thin and dashed lines indicate possible rotation paths characterized by fixed values of γ and δ.

asymmetric in the direction of $\phi=0°$ (180°) with a somewhat steeper incline for $\phi=0°$ and a somewhat flatter incline for $\phi=180°$. This is a direct consequence of the shift of Cl toward C4, which has been explained above. For $\phi=0°$, any increase in δ (γ) moves H of HCl beyond the π density of C4, thus decreasing electrostatic stabilization. A decrease of δ to 0° from the equilibrium position of 14° reduces the complex binding energy by just 0.1 kcal/mol (35 cm^{-1}).

If one assumes just a bending motion of HCl in the mirror plane of the complex, the average value $\langle\delta\rangle$ will be about 11° [$\langle\gamma\rangle=21°$; assuming a bending frequency of about 90 cm^{-1} (Ref. 1)]. However, this estimate does not consider the large libration of the H atom along the half-circle defined by $270°\geqslant\phi\geqslant90°$, which leads to the changes in $\delta(\gamma)$ and ΔE shown in Fig. 7 [$\Delta E(\phi)$ is given by the thick solid line]. With little extra energy the libration of HCl can be converted to an internal rotation. However, in this case the path connecting the gap from $\phi=90°$ to $\phi=270°$ is unspecified. It can lead to the other side of the ring via a form with perpendicular HCl ($\gamma=10°$, $\delta=0°$, barrier: 72 cm^{-1}, Fig. 7) or via the equilibrium form ($\gamma=24°$, $\delta=14°$, barrier: 68 cm^{-1}, Fig. 7), performing in the latter case a ∞-shaped movement over the

plane of the fluorobenzene ring. Also possible is that the δ value of 15.5° ($\gamma=-5.5°$, Fig. 7) is retained and a barrier of 0.27 kcal/mol (94 cm^{-1}) is surmounted.

Since the energy function $E(\delta,\phi)$ was largely determined in this work, it is possible in principle to calculate the zero-point energy level, the wave functions for the two van der Waals vibrations involving δ and ϕ as leading coordinates, and the expectation value $\langle\delta\rangle$ (or $\langle\gamma\rangle$; $\langle\phi\rangle$ is 0°). Because of the asymmetry of the function $E(\delta,\phi)$, this calculation is not trivial and beyond the scope of this investigation. Instead we note that $\langle\gamma\rangle$ values between 11° (internal rotation with fixed δ) and 24° (large amplitude libration) are possible. Considering, in addition, the asymmetry of the PES in the mirror plane, $\langle\gamma\rangle$ can be estimated to be between 16° and 23°. The experimental value of $\gamma=14.5°$ seems to suggest that an internal rotation with largely fixed $\delta=14.7\pm0.7°$ similar as in the benzene–HCl complex ($\delta=14°$[1]) is the most likely internal motion of HCl. The average value $\langle\delta\rangle$ would be about 14.7° if the zero-vibrational level is significantly below the rotational barrier, which in view of the small magnitude of the barrier is not likely. However, if the zero-vibrational level is above the rotational barrier, $\langle\delta\rangle=0.7°$ results, which is in reasonable agreement with the value of 3.8° (Table II) derived from experiment. One has to consider in this connection that the errors in the experimentally derived γ and δ values are relatively large and that the corresponding theoretical values have been just estimated rather than correctly derived quantum mechanically.

VI. CONCLUSIONS

In a two-pronged approach combining high resolution microwave spectroscopy and *ab initio* calculations, the fluorobenzene–HCl complex, which is a prototype for studying changes in π bonding under the impact of a π-donor, σ-acceptor substituent, has been characterized. The following conclusions can be drawn from this investigation.

(1) From the microwave spectroscopic results, the fluorobenzene–HCl complex has been found to possess a vibrationally averaged geometry with the HCl located above the ring, and the hydrogen atom pointing toward the π system of the ring. Large-amplitude motions of the HCl subunit make the determination of the angle between the HCl axis and the perpendicular to the ring difficult. An interpretation of the experimental quadrupole coupling constants has led to an estimate of about 4° (calculated: 0.7°) for this angle. Isotopic substitution data indicate that the Cl atom is shifted slightly from the center of the ring toward C4 (see Fig. 1, model I).

(2) The MP2/6-311++G(2df,2pd)+CP(BSSE) investigation reveals that the π complex is more stable than the σ complex according to calculated complex binding energies. The latter possesses C_{2v} symmetry (HCl in the axis of the CF bond) and is 1.9 kcal/mol less stable. If HCl adopts a position over the ring, it can interact with all heavy atoms while interactions in the ring plane are only possible with the F atom as the only peripheral heavy atom of the ring. Electrostatic attraction between H and the ring atoms is more stabilizing for the π complex than

the σ complex. The latter, however, occupies a local minimum. We note that the spectral search was limited to regions predicted to find the π-bonded complex. A σ complex would lead to quite a different spectrum in a region not yet searched.

(3) The complex binding energy is 2.83 kcal/mol according to CCSD(T)/6-311++G(2df,2pd)+CP(BSSE) calculations. This value suggests that the corresponding complex binding energy for benzene–HCl is in the region $1.8 < D_0 < 3.8$ kcal/mol, as suggested by fluorescence spectroscopy.[5] A complex binding energy of 4.5 kcal/mol, as suggested by recent *ab initio* calculations[1] is definitely too high. In this connection we note that the influence of *d*-type polarization functions at H, *f*-type polarization functions at all heavy atoms, and the infinite-order correlation effects of the CCSD(T) description are decisive for obtaining an accurate complex binding energy.

(4) The complex stability is a result of the best compromise between destabilizing exchange repulsion forces (which are lowest over the center of the ring) and a stabilizing electrostatic attraction between a positively charged H atom and the π density of the ring. Dispersion forces play a minor role.

(5) The complex geometry determined by the three parameters R_{com} [experimental: 3.700 Å, MP2/6-311++G(2df,2pd)+CP(BSSE):3.701 Å], β (100.7°; 100.2°), and γ (14.5°; 16°, Table II, Fig. 1) reflects the π-donor capacity of the F substituent. This increases the π density at C4 and hence enhances the attraction of the H atom by the π density of the ring, provided the Cl atom is shifted by distance u (0.162 Å; 0.116 Å, Table II) toward C4. The shift is a compromise between the enhancement of electrostatic attraction and an increase of exchange repulsion between HCl and the ring. The optimal shift value u depends also on the inclination angle δ, which we find to adopt a similar value in the ground state, as found for benzene–HCl[1] (14°).

(6) π-H bonding in fluorobenzene–HCl is predominantly electrostatic in nature. The charge transfer from the ring to HCl comprises just 5.5 melectron according to a BSSE-corrected NBO analysis in contradiction to predictions made in previous *ab initio* investigations.[9] We conclude that there is only a minor part of the π–H bond due to covalent interactions caused by the overlap between the σ(HCl) MO and the π-MOs of the ring.[1]

(7) HCl performs a large-amplitude libration in the direction described by the phase angle ϕ. However, a change in energy smaller than 100 cm^{-1} suffices to perform an internal rotation similar to that discussed for benzene–HCl. Optimization of δ for different ϕ values reveals that in fluorobenzene–HCl, δ is similar to the value determined for benzene-HCl.[1]

(8) The average values of γ (measured: 14.5°; calculated 16°) and δ (3.8° and 0.7°) could only be estimated in this work. However, both experiment and theory suggest that the most likely motion of HCl is an internal rotation of the HCl bond around the axis Cl-ClP (Fig. 3).

[1] P. Tarakeshwar, S. J. Lee, J. Y. Lee, and K. S. Kim, J. Chem. Phys. **108**, 7217 (1998).

[2] H. S. Gutowsky, E. Arunan, T. Emilsson, S. L. Tschopp, and C. E. Dykstra, J. Chem. Phys. **103**, 3917 (1995).

[3] S. A. Cooke, G. K. Corlett, C. M. Evans, and A. C. Legon, Chem. Phys. Lett. **272**, 61 (1997).

[4] W. G. Read, E. J. Campbell, G. Henderson, and W. H. Flygare, J. Am. Chem. Soc. **103**, 7670 (1981); W. G. Read, E. J. Campbell, and G. Henderson, J. Chem. Phys. **78**, 3501 (1983).

[5] A. J. Gotch and T. S. Zwier, J. Chem. Phys. **93**, 6977 (1990).

[6] F. A. Baiocchi, J. H. Williams, and W. Klemperer, J. Phys. Chem. **87**, 2079 (1983).

[7] E. A. Walters, J. R. Grover, M. G. White, and E. T. Hui, J. Phys. Chem. **89**, 3814 (1985).

[8] Y-H. Zhang, J-K. Hao, X. Wang, W. Zhou, and T-H. Tang, J. Mol. Struct.: THEOCHEM **455**, 85 (1998).

[9] (a) B. V. Cheney and M. W. Schulz, J. Phys. Chem. **94**, 6268 (1990); (b) B. V. Cheney, M. W. Schulz, J. Cheney, and W. G. Richards, J. Am. Chem. Soc. **110**, 4195 (1988).

[10] A. M. Sapse and D. C. Jain, J. Phys. Chem. **88**, 4970 (1984).

[11] W. O. George, Rh. Lewis, G. Hussain, and G. J. Rees, J. Mol. Struct. **189**, 211 (1988).

[12] M. P. Henry and A. N. Hambly, Aust. J. Chem. **20**, 1887 (1967).

[13] D. M. Upadhyay, M. K. Shukla, and P. C. Mishra, J. Mol. Struct.: THEOCHEM **531**, 249 (2000).

[14] C. Petrongolo and J. Tomasi, Int. J. Quantum Chem., Quantum Biol. Symp. **2**, 181 (1975).

[15] R. A. Appleman, S. A. Peebles, and R. L. Kuczkowski, J. Mol. Struct. **446**, 55 (1998).

[16] R. J. Wilson, S. A. Peebles, S. Antolínez, M. E. Sanz, and R. L. Kuczkowski, J. Phys. Chem. A **102**, 10630 (1998).

[17] T. J. Balle and W. H. Flygare, Rev. Sci. Instrum. **52**, 33 (1981).

[18] (a) R. J. McMahon, R. J. Halter, R. L. Fimmen, R. J. Wilson, S. A. Peebles, R. L. Kuczkowski, and J. F. Stanton, J. Am. Chem. Soc. **122**, 939 (2000); (b) J. L. Alonso, F. J. Lorenzo, J. L. López, A. Lesarri, S. Mata, and H. Dreizler, Chem. Phys. **218**, 267 (1997).

[19] (a) W. Gordy and R. L. Cook, *Microwave Molecular Spectra*, 3rd ed. (Wiley-Interscience, New York, 1984); (b) H. M. Pickett, J. Mol. Spectrosc. **148**, 371 (1991).

[20] See EPAPS Document No. E-JCPSA6-118-003320 for Tables S1, S2 (measured transitions) and Table S3 (coordinates). A direct link to this document may be found in the online article's HTML reference section. The document may also be reached via the EPAPS homepage (http://www.aip.org/pubservs/epaps.html) or from ftp.aip.org in the directory /epaps/. See the EPAPS homepage for more information.

[21] (a) S. Doraiswamy and S. D. Sharma, J. Mol. Struct. **102**, 81 (1983); (b) A. C. Legon and D. J. Millen, Proc. R. Soc. London, Ser. A **417**, 21 (1988); (c) A. C. Legon, Faraday Discuss. **97**, 19 (1994); (d) R. H. Schwendeman, in *Critical Evaluation of Chemical and Physical Structural Information*, edited by D. R. Lide and M. A. Paul (National Academy of Sciences, Washington, DC, 1974).

[22] F. H. de Leeuw and A. Dymanus, J. Mol. Spectrosc. **48**, 427 (1973).

[23] (a) C. Møller and M. S. Plesset, Phys. Rev. **46**, 618 (1934). (b) For a recent review, see D. Cremer, in *Encyclopedia of Computational Chemistry*, edited by P. V. R. Schleyer, N. L. Allinger, T. Clark, J. Gasteiger, P. A.

Kollman, H. F. Schaefer, III, and P. R. Schreiner (Wiley, Chichester, UK, 1998), Vol. 3, p. 1706.

[24] K. Raghavachari, G. W. Trucks, J. A. Pople, and M. Head-Gordon, Chem. Phys. Lett. **157**, 479 (1989).

[25] M. A. Spackman, J. Phys. Chem. **93**, 7594 (1989). The 6-31G(+sd,+sp) basis was derived by Spackman by adding to Pople's 6-31G basis (Ref. 27) diffuse polarization functions as well as a diffuse *s*-function. Spackman optimized the exponents of the *d*-type polarization functions for first- and second-row atoms as well as of the *p*-type polarization functions for hydrogen in the way that the mean polarizability of first- and second-row AH_n hydrides is maximized.

[26] Basis 6-31G(d,p): P. C. Hariharan and J. A. Pople, Chem. Phys. Lett. **16**, 217 (1972).

[27] Basis 6-311++G(2df,2pd): R. Krishnan, M. Frisch, and J. A. Pople, J. Chem. Phys. **72**, 4244 (1980).

[28] For a review on the basis set superposition problem, see F. B. van Duijneveldt, J. G. C. M. van Duijneveldt-van de Rijdt, and J. H. van Lenthe, Chem. Rev. **94**, 1873 (1994).

[29] J. J. Oh, I. Park, R. J. Wilson, S. A. Peebles, R. L. Kuczkowski, E. Kraka, and D. Cremer, J. Chem. Phys. **113**, 9051 (2000).

[30] (a) E. Kraka, D. Cremer, U. Spoerel, I. Merke, W. Stahl, and H. Dreizler, J. Phys. Chem. **99**, 12466 (1995); (b) U. Spoerel, H. Dreizler, W. Stahl, E. Kraka, and D. Cremer, *ibid.* **100**, 14298 (1996).

[31] S. F. Boys and F. Bernardi, Mol. Phys. **19**, 553 (1970).

[32] (a) J. E. Carpenter and F. Weinhold, J. Mol. Struct.: THEOCHEM **169**, 41 (1988); (b) A. E. Reed, R. B. Weinstock, and F. Weinhold, J. Chem. Phys. **83**, 735 (1985). (c) A. E. Reed, L. A. Curtiss, and F. Weinhold, Chem. Rev. **88**, 899 (1988).

[33] E. Kraka, J. Gräfenstein, J. Gauss, F. Reichel, L. Olsson, Z. Konkoli, Z. He, Y. He, and D. Cremer, COLOGNE2000, Göteborg University, Göteborg, 2000.

[34] (a) J. F. Stanton, J. Gauss, J. D. Watts, W. J. Lauderdale, and R. J. Bartlett, ACES II, Quantum Theory Project, University of Florida, 1992. (b) See also J. F. Stanton, J. Gauss, J. D. Watts, W. J. Lauderdale, and R. J. Bartlett, Int. J. Quantum Chem., Symp. **26**, 879 (1992).

[35] P. Salvador, S. Simon, M. Duran, and J. J. Dannenberg, J. Chem. Phys. **113**, 5666 (2000).

[36] P. Tarakeshwar, K. S. Kim, E. Kraka, and D. Cremer, J. Chem. Phys. **115**, 6018 (2001).

[37] E. Kraka, D. Cremer, and R. L. Kuczkowski, (unpublished).